

Transition to a time-dependent state of fluid flow in the wake of a sphere

K. Gumowski and J. Miedzik

Warsaw University of Technology, Institute of Aeronautics and Applied Mechanics, ul. Nowowiejska 24, 00-665 Warsaw, Poland

S. Goujon-Durand, P. Jenffer, and J. E. Wesfreid

PMMH – ESPCI, CNRS UMR 7636, 10, rue Vauquelin, 75231 Paris Cedex 05, France

(Received 5 December 2007; published 30 May 2008)

In this paper, the results of laboratory investigation about the flow behind the sphere in the range of $150 < \text{Re} < 300$, where very interesting physical phenomenon occurs, are presented. After a first stationary transition where the flow breaks the axisymmetry, very controlled experiments allow one to define a threshold for the second transition from stationary to unstable flow, which includes three-dimensional peristaltic oscillations of the two trailing vortices prior to hairpins shedding. The scenario has been proposed to explain the hairpin formation, as pieces of a counter-rotating longitudinal vortex. Hairpin shedding is suggested to be the result of oscillations, which are powerful enough, and reconnection of the trailing vortices.

DOI: [10.1103/PhysRevE.77.055308](https://doi.org/10.1103/PhysRevE.77.055308)

PACS number(s): 47.15.-x

The wake behind the sphere has been the object of a large number of experimental and numerical studies and is one of the prototypes of flow around three-dimensional (3D) bodies. Previous works [1–3] distinguish different flow regimes behind the sphere. From rest up to Reynolds number $\text{Re}=20$ fluid swims around the sphere and rest without recirculation area [4]. The wake of the sphere has an axisymmetric stationary ring structure which keeps its axisymmetry with increasing Reynolds numbers up to $\text{Re}=212$. At $\text{Re}=212$, this axisymmetry of the recirculation zone is broken and the flow undergoes a first stationary bifurcation and two parallel steady counter-rotating vortices appear. In contrast to the flow behind cylinder, which after the first bifurcation becomes unsteady, flow behind the sphere shows a steady stability.

As shown in most numerical and experimental works [3,5–7] this second transition from a stable to a time-dependent flow occurs at the $\text{Re} \sim 275$, and the unsteady wake is characterized by the periodic shedding of connected hairpin vortices. For Reynolds numbers higher than 350, the shedding changes its character. Two small hairpins follow one larger hairpin. At $\text{Re} \sim 500$ the flow becomes chaotic.

In spite of the geometrical simplicity of the sphere, the vortices structures developing behind this bluff body are difficult to describe, e.g., first bifurcation transition with the apparition of two-tailed wake, the mechanism of hairpins appearance, developing and the hairpins connection are not well known and until today they remain not fully described. This problem is of enormous importance as this flow is a good prototype to understand the global problems of instabilities in inhomogeneous flows, which are the subject of intense modern developments. In addition the instability of the trailing vortices is an academic subject of renewed interest with the application in aeronautics, related to the problem of vortex reconnection or with the problem of the persistence of two trailing vortices limiting seriously the frequency of landing in airports. The existence of this instability are intensively studied in bubbles motion where this problem is observed and is known as the Leonardo da Vinci paradox.

So in this work the exact mechanism driving the transition to unsteady flow was studied. In the experiments the focus

was on the investigation of flow around a second bifurcation, numerically studied previously by Johnson and Patel [2] and Tomboulides and Orszag [7].

All experiments were carried out in a low velocity water channel with a square cross section ($10 \times 10 \text{ cm}^2$) and 86 cm long, which for the sphere of diameter $d=1.6 \text{ cm}$, is longer than 50 sphere diameters. The sphere was held from upstream by a rigid bent tube with negligible perturbation on the flow, but capable of determining the plane of the mirror symmetry. Velocity in the water tunnel was deduced from flow mass rate measurement with a special developed strain gauge balance. Typical velocities were 0.4 to 4 cm/sec, which corresponds to a Reynolds number from 63 up to 630. The water temperature was measured with a precision $\pm 0.1^\circ$.

The wake visualizations were performed using laser induced fluorescence (LIF) or ink. The dye is injected without significant influence on the recirculation bubble in the middle of the sphere by using a thin slit (Fig. 1) of controllable horizontal or vertical orientation.

Particle image velocimetry (PIV) image acquisition and postprocessing were done using ImagerPro 1600×1200 12-bit charge-coupled device (CCD) camera recording double-frame pairs of images at 15 Hz and a two rod Nd:yttrium-aluminum-garnet (Nd:YAG) (15 mJ) pulsed laser all synchronized by the customized PC (using LaVision DaVis software).

The main interest of the studies was to define exactly the

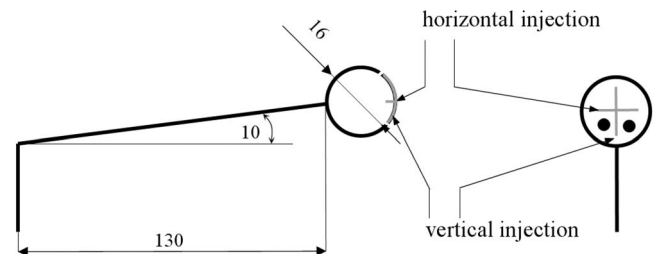


FIG. 1. Scheme of the holding of the sphere, including dye injection principle. The black points on the right show schematically the position of two counter-rotating vortices. Left picture is side view; right picture is rear view.

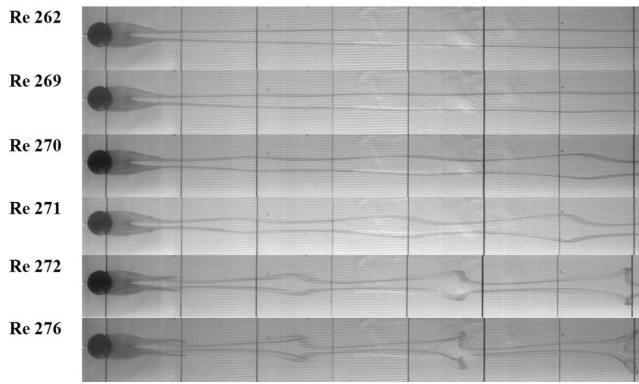


FIG. 2. Oscillations evolution (top view photos).

beginning and the nature of the second transition from the stationary state with two counter-rotating vortices to hairpin vortex shedding. In the previous studies, it was assumed that after a steady stationary flow with two counter-rotating vortices, hairpin shedding appears as a consequence of a bifurcation. Previous publications [1,2] indicate that the second threshold occurs for $Re=275$. Most authors suggest this threshold as a change from a stable planar symmetrical regime with two counter-rotating vortices to an unstable regime or Hopf bifurcation with regular hairpin shedding phenomenon, without emphasizing oscillations prior to hairpin development.

We began to observe the flow from $Re=240$ to $Re=300$. During the present experiments it was observed that small kinks appear prior to hairpins shedding (Fig. 2). Similar behavior can be observed in visualizations presented by Schouveiler and Provansal [4] (also [3,6,7]) and is seen in numerical studies by Thompson [5].

The two vortices are positioned behind the sphere. Because the vortices produce downwash, the line which joins the vortices cores does not lie on the diameter but it is situated under the middle of the sphere, which can be seen in Fig. 1.

The visualizations pattern (photos taken from the top) of the flow behind the sphere is shown in Fig. 2. These two streaklines correspond to two longitudinal counter-rotating vortices which are steady up to $Re=265$. Starting from Reynolds number around 267 it is easy to notice, by visualization, small periodic deformation of the two counter-rotating vortices in the wake of the sphere. The amplitude of the modulation of the streaklines grows with the increase in the Reynolds number. First modulations are perceptible in the far wake of the sphere (these first detectable oscillations in the

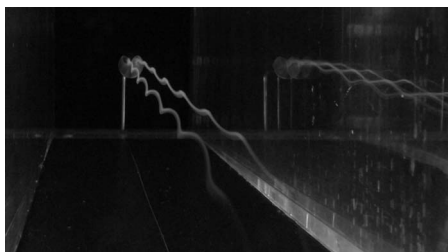


FIG. 3. Beginning of peristaltic oscillations, rear view.

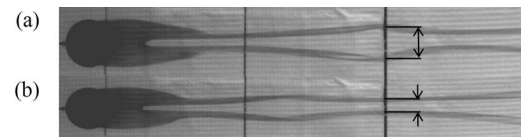


FIG. 4. Δ definition, on (a) and (b) are shown ways of measuring b' and b'' , respectively, $\Delta=b''-b'$.

top view are in the far wake) and after increasing the Reynolds number are observable in whole wake behind the sphere. This flow is not stationary anymore. The amplitude of the oscillations grows with the distance downstream from the sphere.

The observed streaklines of oscillating vortices seem to have a spiral form (Fig. 3). It is important to emphasize that this phenomenon is fully three dimensional. These deformations are observed in two perpendicular planes. For example, the biggest deformation in the xz plane corresponds to the lowest position of the vortices in the yz plane if the two initial vortices are positioned in the lower half of the yz plane. The vortices are not lying in a horizontal or vertical plane nor any other plane.

Further increasing the Reynolds number, one reaches the point of observable hairpins shedding, which occurs at Reynolds number of about 280.

To measure the amplitude of the oscillations, a Δ parameter was defined as the difference between the biggest b'' and the shortest b' distance between vortices cores (Fig. 4), and it was measured on the top view photos. Each photo series to measure the Δ parameter was taken with a very small increment of Reynolds number in comparison to the previous series.

As shown in Fig. 5 the Δ value is growing with the distance downstream from the center of the sphere, which correlates with the distance between cores in the stationary regime, which is also growing with the distance downstream from the center of the sphere. The Δ parameter increases almost linearly with Reynolds numbers in the range of 269 to 278. For the Re numbers higher then 278 the value of the Δ reaches saturation. From linear approximation and extrapolation for all distances downstream from the center of the sphere, the Δ reaches the zero value at $Re=267$. The estimated instability onset can be established at $Re=267$, as for

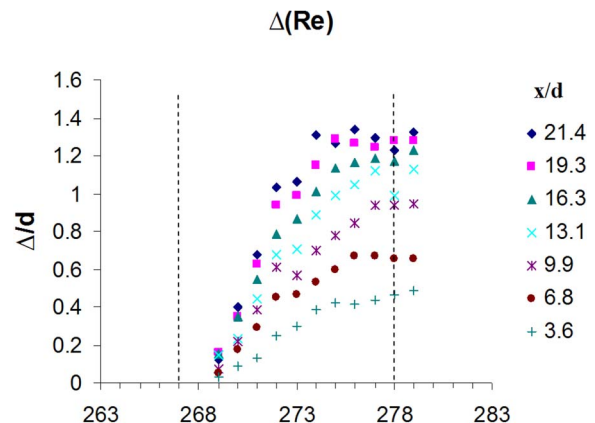


FIG. 5. (Color online) Δ as a function of Reynolds number.

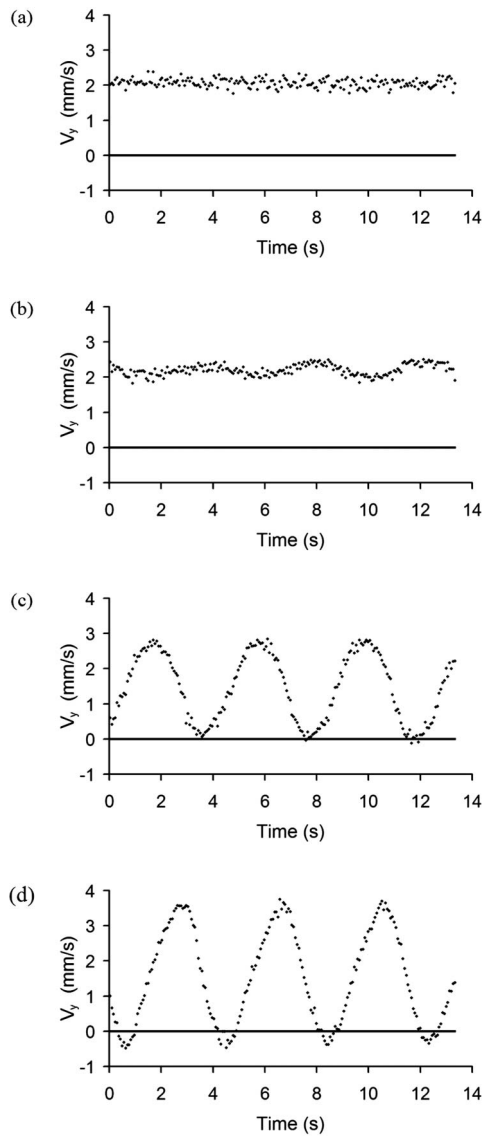


FIG. 6. V_y velocity component oscillations for Reynolds numbers 262 (a), 266 (b), 280 (c), 291 (d). For Re 280 (c) the velocity crosses zero value, which corresponds to hairpins appearance.

this Reynolds number the wake becomes modulated and instationary. At this value the onset of the second instability is defined as a 3D peristaltic oscillation which modulates the two counter-rotating vortices.

The investigation of flow around this second threshold obtained by visualization are confirmed below with the results of PIV measurements. In order to obtain more information about hairpins development a time-dependent parameter was chosen. The parameter was the vertical velocity component V_y in the area between vortices. In addition a spatial average \overline{V}_y component was defined as

$$\overline{V}_y = \frac{1}{S} \int V_y dy dz$$

on a small region $[y, z]$ between two trailing vortices. The calculation area is the same on each image (the area is cho-

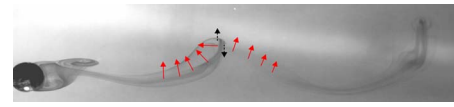


FIG. 7. (Color online) Visualizations of hairpins shedding; black dotted arrows hairpins head velocity, red arrows between vortices velocity.

sen arbitrary; the limits have no influence on the measured frequency). The series includes 200 images, each taken at the frequency of 15 Hz.

At $Re=262$ the plot of the velocity component V_y between cores is constant in time and noisy (see Fig. 6). With an increasing Reynolds number the harmonic fluctuations are noticed at the value of $Re=266$. These fluctuations are related to the kinking phenomenon and the amplitude is growing with an increasing Re number. The value of V_y velocity is always positive in time.

At $Re=280$, the measured spatial average velocity \overline{V}_y reaches the value zero for what is shown in Fig. 6. The value of zero vertical velocity is the result of the appearance of the closed vortex loops, hairpins (Fig. 7). Transverse component of vorticity produced by the hairpin head induces downwash flow periodically in the plane of measurement. It is clear that when both two counter-rotating vortices are straight lines or are even kinking the velocity between them is always directed in one way, in our case is still directed upwards (due to the holding influence). The vertical velocity component equals zero the first time when the hairpins are produced. The hairpin head is spinning in the direction perpendicular to the rest of the hairpin so the velocity produced by the hairpin head on one side of its center is in opposition to “between-vortices” velocity. Moreover the vertical velocity component V_y in the center of the hairpin head is zero. It is the center of the vortex. Because the hairpin is not laying in one plane but is curved, the induced velocity “between vortices” changes direction from vertical to horizontal, which is probably the main reason of the zero value of vertical velocity (Fig. 7). The first hairpin appearance at $Re=280$ can be considered as a result of oscillations strong enough, as well as the undulated longitudinal vorticity.

Unstable phenomena are characterized by their own frequencies. As shown in Fig. 8 the frequencies of peristaltic instability and of the hairpins shedding (measured by PIV

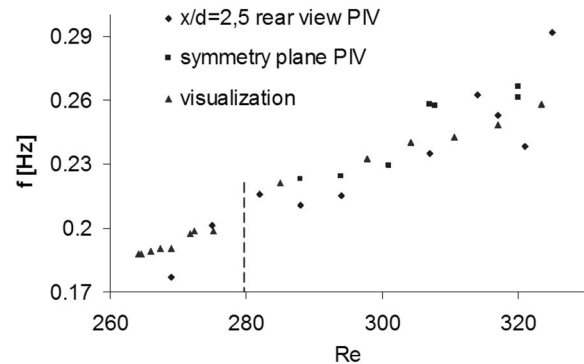


FIG. 8. Frequency of 3D peristaltic instability and hairpins shedding.

rear and side images and confirmed by visualizations) are laying in the same line which implies that the hairpins shedding frequency is a continuation of 3D peristaltic undulation frequency. It means that both these phenomena are related to the same instability. This instability already starts at the Reynolds number around $Re=266$. It seems that the hairpin is just the result of sufficiently strong oscillations in the wake, more precisely in the recirculation area, and appears as a large amplitude modulation and reconnection which should be further studied.

A view on the hairpins formation onset is presented in the work. Hairpins are essentially small pieces of counter-rotating vortices produced by stages of strong modulation and reconnection of the two marginal longitudinal vortices produced on the nonaxisymmetrical recirculation loop. Consequently the real instability is the one observed in our experiment starting from $Re=265$, which we call 3D peristaltic

instability and which is reminiscent of the Crow instability [8] occurring from vortices of high circulation which is widely studied in aeronautics. But, the Crow instability produces oscillations of vortices in two planes inclined at 43° and the streaklines here are 3D (Fig. 3).

In the second regime, the wake behind the sphere is characterized by two counter-rotating vortices, similar to the wing tip vortices behind an airplane, which prolong the time between individual take offs and landings of the planes. The sphere is the simplest natural generator of two counter-rotating vortices that allows the study of elementary interactions between vortices.

The authors acknowledge the French Embassy for a scientific grant, and thank R. Godoy-Diana and A. Prządka for collaboration.

-
- [1] R. H. Magarvey and R. L. Bishop, *Can. J. Phys.* **39**, 1418 (1961).
[2] T. A. Johnson and V. C. Patel, *J. Fluid Mech.* **378**, 19 (1999).
[3] D. Ormières, Ph.D. thesis, Université de Provence, 1999.
[4] L. Schouveiler and M. Provansal, *Phys. Fluids* **14**, 3846 (2002).
[5] M. C. Thompson, T. Leweke, and M. Provansal, *J. Fluids Struct.* **15**, 575 (2001).
[6] D. Ormières and M. Provansal, *Phys. Rev. Lett.* **83**, 80 (1999).
[7] A. G. Tomboulides and S. A. Orszag, *J. Fluid Mech.* **416**, 45 (2000).
[8] S. C. Crow, *AIAA J.* **8**, 12 (1970).